Chapter 3 - Capacitive Joining and Assembly of Bulk Metallic Glass Matrix Composites

Strong, robust joining of metal components is a key consideration in the fabrication of complex assemblies and consumer products. Developing optimal welding and joining practices for each class of materials is critical for their integration into products. Bulk metallic glasses (BMGs) are a relatively new class of materials with exceptional mechanical properties. However, they lack an obvious joining process, owing to their unique amorphous microstructure. BMGs are known for their combination of ultra-high strength, high hardness, large elastic limit, and low melting temperatures that allow them to be cast or molded like polymers. These properties have been widely exploited in applications such as electronic cases and golf clubs, but have been mostly relegated to small, near-net shape parts that are components of larger structures. This is due to a number of factors, including the difficulty of casting larger parts, material cost, and the low toughness of BMGs. Recently, a new class of BMG composites has emerged with soft crystalline dendrites. These dendrites allow the material to deform plastically (up to 10% elongation prior to failure), resulting in a material with ultra-high toughness that still preserves the strength of the metallic glass.[1] These alloys have been semi-solidly processed into panels and cellular structures and been shown to possess some of the highest energy-absorbing capacities of any metal structure.[2,3] Panels of the current BMG composites are already under investigation in energy-absorbing applications, such as orbital debris shielding for spacecraft and satellites, crushable landing foams for extra-terrestrial rovers, and as panels on military vehicles and vessels.[4] The ability to weld these structures together to form wider panels or thicker cellular structures is alluring for future structural applications. Similarly, the ability to weld monolithic BMGs, especially in small parts, has the potential for greatly enhancing their functionality in commercial applications. In this chapter, it is demonstrated that by flash heating and cooling joints of BMGs or BMG composites using capacitive discharge, unions can be achieved with properties nearly indistinguishable from the parent material, opening up the possibility for continuous BMG structures to be fabricated from multiple pieces.

Currently, the joining of BMGs in commercial hardware is eschewed in favor of casting net-shape parts that can then be snapped or bonded together with epoxy. Conventional welding or joining techniques used for many crystalline metals are difficult to apply to BMGs because high rates of cooling are required to vitrify the part. Therefore, any joining operation must both heat and cool the metal quickly, as any heat affected zone (HAZ) reaching temperatures in excess of the glass transition is in danger of crystallization. Many techniques have been attempted for welding BMGs, including friction welding, friction-stir welding, explosive welding, electron beam welding, and laser joining.[5–8] Friction welding, where samples are generally rotated together to generate enough frictional heating to allow for joining, requires samples with axial symmetry, as well as finish-machining operations to remove flashing. Friction stir welding, which involves insertion and translation of a rotating pin tool to mechanically stir material into a welded region, is typically limited to butt welds (although NASA has used the technique for orbital welding of rocket bodies) and has low cooling ability unless the sample is submerged.[9] Explosive welding is not practical for precise joining of parts. While laser welding is very precise, the required dwell time of the laser is long, and results in cooling rates slow enough to crystallize all but the most robust glass formers.

To practically weld BMGs (and, by extension, BMG composites) with precision, a method is needed to rapidly heat and join two BMG interfaces while retaining the ability to quench the HAZ faster than the critical cooling rate for glass formation. One solution involves the use of electrical current pulses, and associated Joule heating, to rapidly heat and join BMG parts while allowing the part to be quickly cooled through conduction and radiation. This technique has been used previously to cut and shear metallic glass ribbons,[10] rapidly anneal ferromagnetic metallic glass ribbons,[11] and to weld rods (in what can be considered the precursor to the present work)[12,13]. Spot welding of metallic glass sheets has been demonstrated as a feasible way of forming a joint with up to 70% of the yield strength of the parent material without any detectible crystallization.[14] Recently, Johnson et al. have demonstrated that high imposed current densities and ohmic dissipation can be used for uniform volumetric heating of BMG samples to temperature ranges where they can be processed through injection casting.[15] This was accomplished by discharging energy from a capacitor bank into a cylindrical rod of a BMG and then injecting the softened glass into a mold using the upper electrode as a plunger. In contrast, the present work focuses on welding structures by passing a large current density through the junction between two BMG parts, where the upper electrode provides a sufficiently high compression load to join the heated interface. Because the load required for joining is far lower that the load required for injection molding, complex electrode geometries can be developed which allow for "projection" welding of BMG parts (see Figure 3-1(b-c) for an example). In the current work, this technique is demonstrated to not only form a union with strength approaching that of the parent material, but also to form complex cellular structures that do not preferentially fail at the joints.

To demonstrate the strength of the weld created with this technique, the BMG composite DH1 ($Zr_{36.6}Ti_{31.4}Nb_7Cu_{5.9}Be_{19.1}$) was selected. This alloy comprises a highly processable glassy matrix[16] and approximately 40% volume fraction of soft, body centered cubic crystals embedded homogeneously throughout. The alloy was suction cast into stepped plates

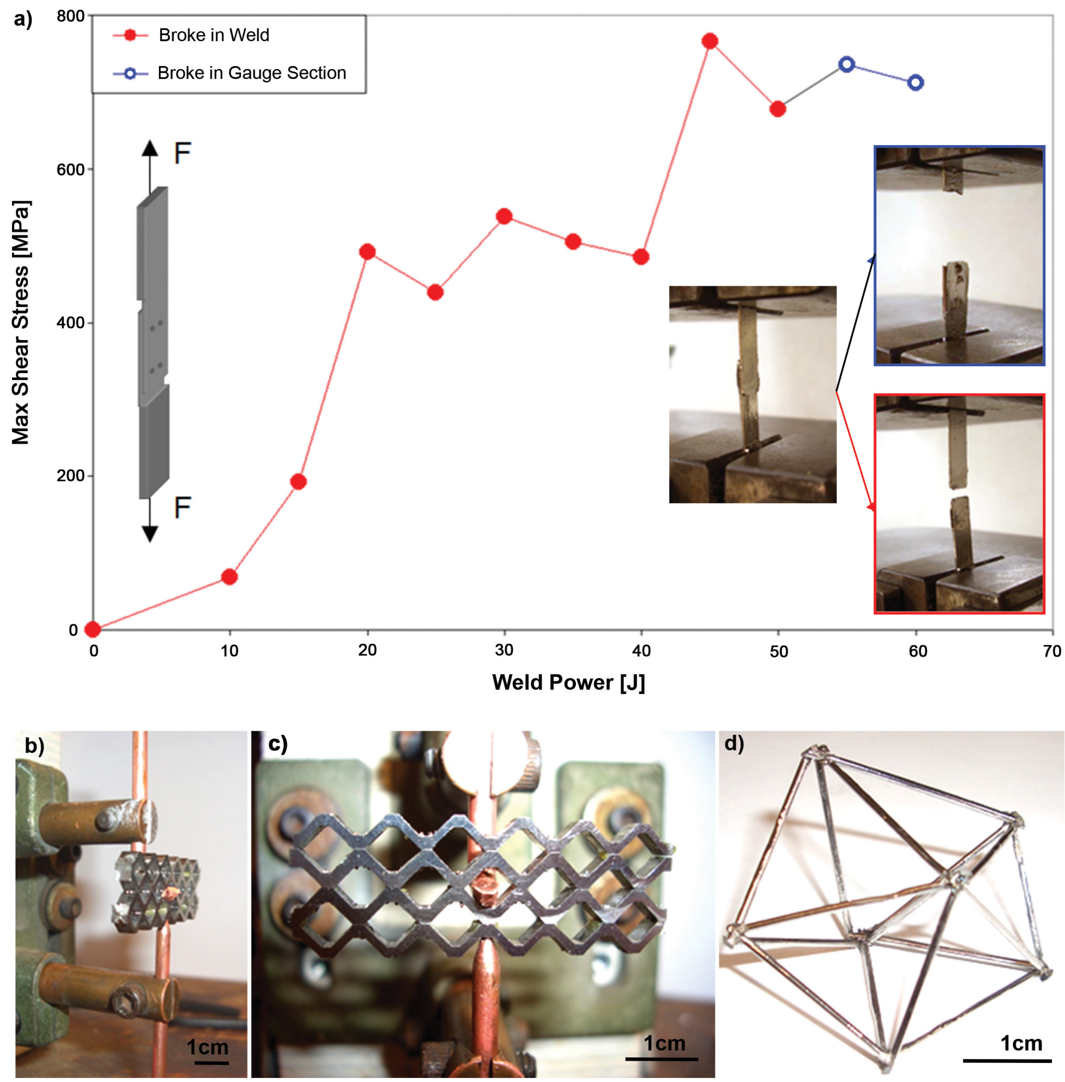

Figure 3-1: (a) Maximum shear stress versus welding power for plates of the BMGMC DH1 that were subjected to four welds for each power. The schematic shows that the geometry of the plates was designed so that the tension test applies pure shear to the welded regions. The red solid circles represent failure in the welds while the filled blue circles represent failure outside the welded region. (b-c) Examples of how copper electrodes can be bent to do "projection welding." In this case, a square honeycomb of the BMGMC DH1 is welded together from corrugated strips. (d) A truss welded fabricated by welding together 1 mm diameter rods of the BMGMC DH1 at the nodes.

(5x30 mm) with a thickness of 1mm on one side, and a thickness of 0.5mm on the other. Two plates were overlapped and welded such that the total thickness of the welded part was 1 mm throughout. This geometry was selected so that a uniaxial tension test could be used to approach a condition of pure shear in the welded region (inset of Figure 3-1a). To join the plates, two copper electrodes were polished to have a 1 mm diameter flat tip. The plates were spot welded using energies ranging from 10 to 70 J per discharge from the capacitor bank. Four welds were used to join each set of plates (leading to a total welded area of ~13 mm^2); the samples were then pulled in tension at a strain rate of 0.1 mm/min until failure. Figure 3-1a shows a plot of capacitor discharge energy versus shear stress at failure. A clear trend of increasing maximum shear stress with increasing weld power was observed until a stress plateau was reached at approximately 500 MPa. At weld energies above 40 J, there appears a jump in the shear stress at failure, leading to a second plateau around 700 MPa, which is approximately the lower bound on the maximum yield strength of the parent material, DH1. The amount of flow and lack of weld line at these discharge energies indicates that a temperature above the solidus was reached (970 K for DH1); however, since the size and morphology of the dendrites appear unaltered at all welding powers, the dwell time or the elevated temperature were insufficient to melt the dendrites (Figure 3-2). With weld energies greater than 50 J, the strength of the welds matches or exceeds the tensile strength of the 0.5x3 mm cross-section of the parent material, and failure occurs in the gauge section instead of along the welds. SEM and XRD inspection of the fracture surface shows no indication of crystallization. At high welding power, the observed shear strength of the welded samples is approximately the same as the yield strength of the plate (τ_y = 700 MPa), demonstrating the ability to form a welded joint with the same mechanical strength as the parent material. It should be noted that these experiments were replicated using a comparable monolithic BMG, and the results showed a similar trend (data not shown).

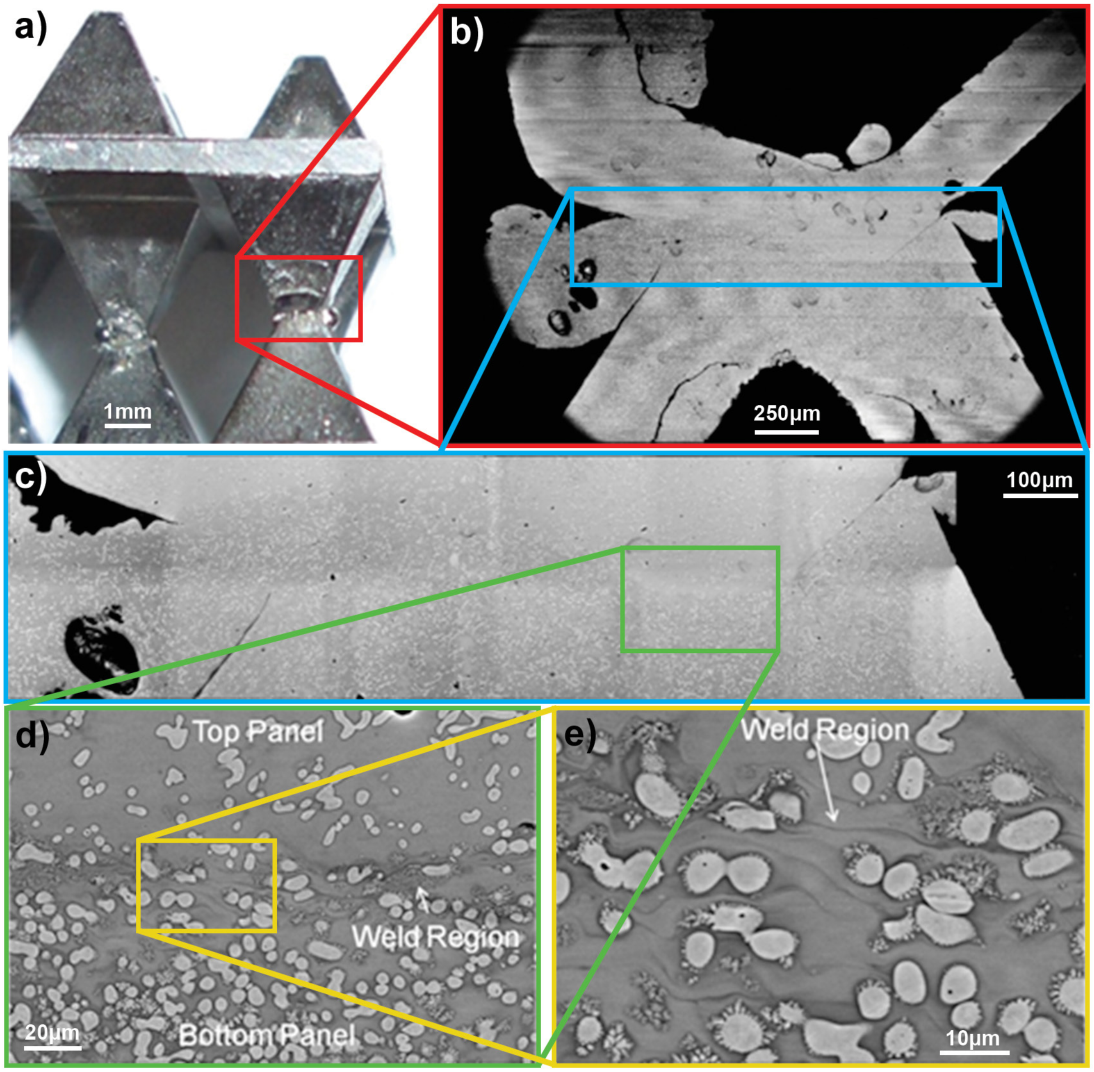

Figure 3-2: (a) An optical image of the nodes between two welded DH1 egg-boxes showing the extent of flow during the welding. (b-e) Progressively enlarged SEM micrographs showing the microstructure of the welded regions. The low magnification micrograph in (b) shows the that material has flowed from under the welding electrodes. At higher magnification (c) there is a clear seam between the two welded pieces that disappears in the location under the electrodes, indicating a solid weld. (d-e) Enlargements of the weld region showing flow lines from the joining but also showing dendrites that were unaffected by the flowing glass matrix. The weld is comprised on the glass matrix from each sample having been heated and joined under the compressive loads without the dendrites being affected. The dendrite microstructures in (d-e) are nominal for the sample outside the welded region.

The key advantage of the capacitive welding technique is the ability to assemble and join BMG composite cellular structures into geometries that cannot be fabricated using other techniques (due to blind machining features, for example). To demonstrate this, panels of semi-solidly forged BMG composite egg-boxes were stacked and welded into cellular structures, and then loaded in compression. The egg-box geometry, which was developed by Schramm et al.[17] for BMG composites, is an elegant way of fabricating a cellular structure that has nearly isotropic deformation in the x-y plane and can be made easily using interlocking molds. Panels with wall thicknesses of 0.5-0.8 mm were produced by semisolid forging,[3] and were demonstrated to have among the highest energy absorbing capacity of any cellular structure.[17] Moreover, the geometry of the egg-box allows for stacking, since the 1 mm square top of each pyramidal cell is designed to align with the bottom of the adjacent cell. Samples were sectioned into 3x3 cells, and the tip of each pyramid was polished. The samples were then stacked, clamped, and the joints were welded together. Two sets of 3x3x2 structures were fabricated at weld energies of 20 J and 40 J. A representative welded sample was cross-sectioned, polished, and imaged using an SEM in QBSD mode to observe the character of the weld (Figure 3-2). As expected, the welding process did not provide sufficient heating or dwell time to allow for the dendrites to go into solution. The dendrite morphology and volume fraction inside the welded region was identical in appearance to the parent material, which was formed through semi-solid forging. Not only was there a continuous path of BMG matrix through the HAZ, but significant flow from both sides of the weld was observed. This indicates that heat generated by the discharge was sufficient to lower the viscosity of the sample, allowing for flow, while the compressive force from the electrode was sufficiently large to induce mechanical mixing between the two sides of the junction. Despite the significant amount of overflow, the dendrites

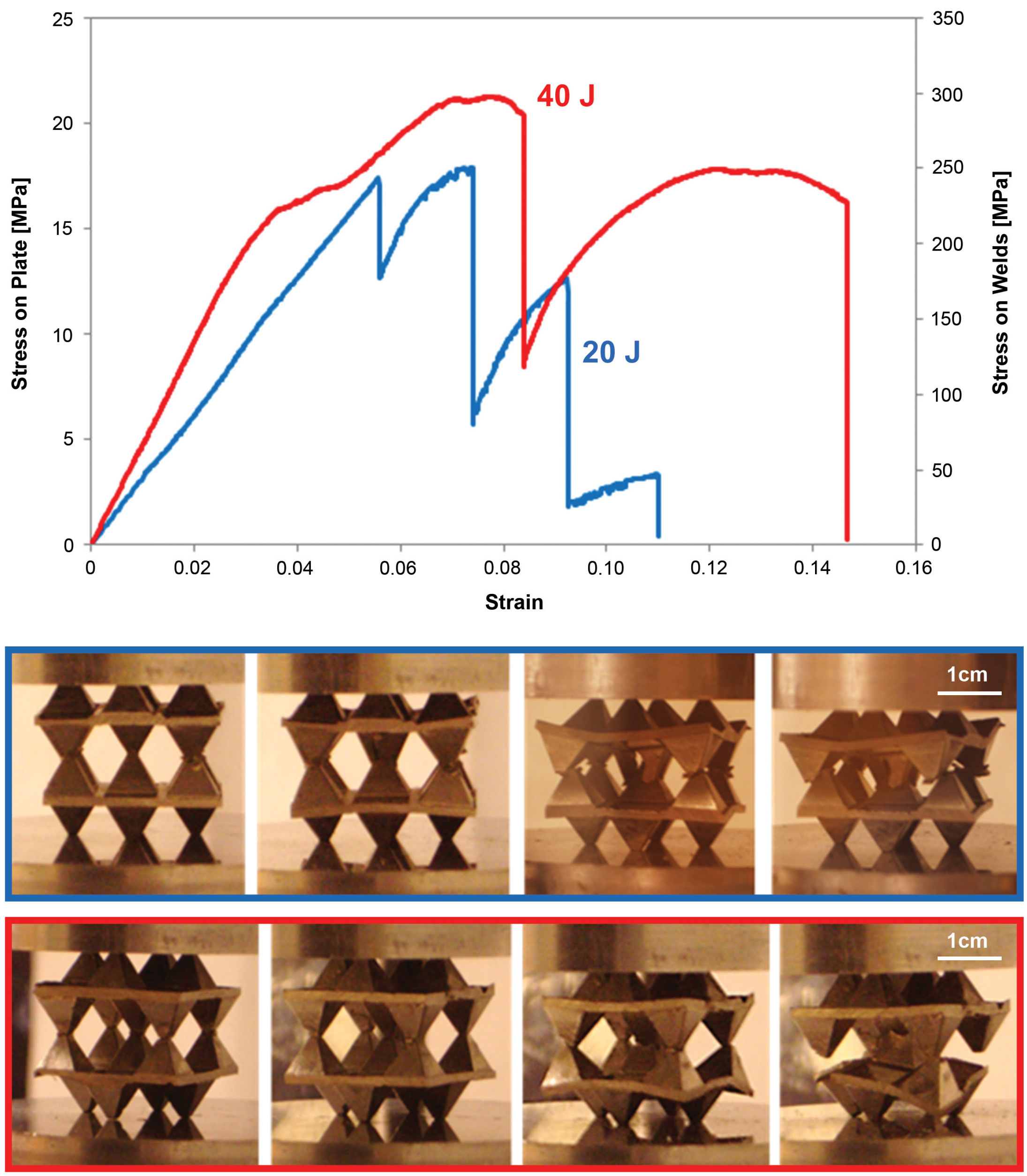

Figure 3-3: Quasistatic compression testing of two DH1 egg-boxes that were welded together at five locations. The blue curve represents a welding power of 20 J (pictured on top) while the red curve represents 40 J (pictured on bottom). Under compression, the samples experience a mixed-mode buckling from edge effects which ultimately breaks the weld. At 40 J, there is a significant amount of buckling before the weld fails, indicating a higher quality weld. This is verified by the compression data, which shows a higher energy absorption in the 40 J welded samples.

were merely displaced by the process and did not have time to change morphology. Moreover, a combination of thermal radiation into the air, conduction into the sample, and conduction into the copper electrodes provided a sufficient cooling rate to prevent the welded junction from crystallizing. This demonstrates that a continuous joint between two pieces of a BMG composite can be created; resulting in a single, uniform structure unobtainable by conventional casting techniques.

By utilizing this projection welding technique, nxn cellular structures can be fabricated from panels of tough, energy absorbing BMG composites. The strength of the welded junction and the energy absorbing capacity of the two-layer, 3x3, welded egg-boxes were assessed using quasi-static compression tests (Figure 3-3). Two samples, welded at 20 J and 40 J, were loaded until failure. The sample welded using 40 J of energy withstood substantially higher loads, and absorbed more energy than the structure welded at lower power. Both samples failed at the welded junctions, primarily due to torque from edge-effects in the samples (Figure 3-3(d-e)).

One potential application of the current technology is the welding of multiple layers of egg-boxes into a thick cellular structure (i.e. an ordered foam). However, with the addition of a third layer, a direct line-of-sight from the welded junction to the electrodes is lost. This can be solved by utilizing a projection welding configuration where the copper electrodes can be bent into complex shapes and inserted into the space between each layer (Figure 3-1(b-c)). Large, truss-like structures were also fabricated out of thin rods using this technique (Figure 3-1d).

The rapid heating and cooling obtained through the use of capacitive welding techniques represent a paradigm shift in the way that BMGs and BMG composites can be integrated into parts. Unlike conventional welding, where the HAZ contains material that is fundamentally different in microstructure and mechanical properties from the parent material, capacitive welding allows for joining BMGs without altering the microstructure. This enables the manufacture of complex parts that could not otherwise be fabricated using any conventional technique. Furthermore, the joints created with this technique exhibit the strength of the parent material, resulting in a structure that behaves as though it was made from a monolithic material. In the next chapter, we show that welding together cellular structures from BMGMCs results in excellent ballistic performance as orbital debris shields for spacecraft.

Citations

[1] D.C. Hofmann, J.-Y. Suh, A. Wiest, M.-L. Lind, M.D. Demetriou, and W.L. Johnson, Proc. Natl. Acad. Sci. U. S. A. **105**, 20136 (2008).

[2] M. Demetriou, C. Veazey, J. Harmon, J. Schramm, and W. Johnson, Phys. Rev. Lett. **101**, 145702 (2008).

[3] D.C. Hofmann, H. Kozachkov, H.E. Khalifa, J.P. Schramm, M.D. Demetriou, K.S. Vecchio, and W.L. Johnson, JOM **61**, 11 (2009).

[4] M. Davidson, S. Roberts, G. Castro, R.P. Dillon, A. Kunz, H. Kozachkov, M.D. Demetriou, W.L. Johnson, S. Nutt, and D.C. Hofmann, Adv. Eng. Mater. n/a (2012).

[5] H.-S. Shin, J.-S. Park, and Y. Yokoyama, J. Alloys Compd. **504**, S275 (2010).

[6] Y. Kawamura, Mater. Sci. Eng. A **375-377**, 112 (2004).

[7] Y. Kawamura, T. Shoji, and Y. Ohno, J. Non. Cryst. Solids **317**, 152 (2003).

[8] H.S. Wang, H.G. Chen, J.S.C. Jang, and M.S. Chiou, Mater. Sci. Eng. A **528**, 338 (2010).

[9] D.C. Hofmann and K.S. Vecchio, Mater. Sci. Eng. A **402**, 234 (2005).

[10] D.E. Ballard, P.G. Frischmann, and A.I. Taub, U.S. Patent No. 5005456 (9 April 1991).

[11] M. Vázquez, J. González, and A. Hernando, J. Magn. Magn. Mater. **53**, 323 (1986).

[12] Y. Kawamura and Y. Ohno, Scr. Mater. **45**, 127 (2001).

[13] a. R. Yavari, M.F. de Oliveira, C.S. Kiminami, a. Inoue, and W.J. Botta F, Mater. Sci. Eng. A **375-377**, 227 (2004).

[14] K. Fujiwara, S. Fukumoto, Y. Yokoyama, M. Nishijima, and A. Yamamoto, Mater. Sci. Eng. A **498**, 302 (2008).

[15] W.L. Johnson, G. Kaltenboeck, M.D. Demetriou, J.P. Schramm, X. Liu, K. Samwer, C.P. Kim, and D.C. Hofmann, Science **332**, 828 (2011).

[16] G. Duan, A. Wiest, M.L. Lind, J. Li, W.-K. Rhim, and W.L. Johnson, Adv. Mater. **19**, 4272 (2007).

[17] J.P. Schramm, D.C. Hofmann, M.D. Demetriou, and W.L. Johnson, Appl. Phys. Lett. **97**, 241910 (2010).